Hypothesis tests for the detection of constant speed radiation moving sources

Jonathan Nicolas Dumazert, Romain Coulon, Vladimir Kondrasovs, Karim Boudergui, Guillaume Sannié, J. Gameiro, Stéphane Normand, Laurence Méchin

Hypothesis tests for the detection of constant speed radiation moving sources

Jonathan Dumazert, Romain Coulon, Vladimir Kondrasovs, Karim Boudergui, Guillaume Sannié, Jordan Gameiro, Stéphane Normand and Laurence Méchin.

***Abstract*–As a complement to single and multichannel detection algorithms, inefficient under too low signal-to-noise ratios, temporal correlation algorithms have been introduced to detect radiological material in motion. Test hypothesis methods based on the mean and variance of the signals delivered by the different channels have shown significant gain in terms of a tradeoff between detection sensitivity and false alarm probability. This paper discloses the concept of a new hypothesis test for temporal product detection methods, taking advantage of the Poisson nature of the registered counting signals, and establishes a benchmark between this test and its empirical counterpart. The simulation study validates that in the two relevant configurations of a pedestrian source carrier under respectively high and low count rate radioactive backgrounds, the newly introduced hypothesis test ensures a significantly improved compromise between sensitivity and false alarm, while guaranteeing the stability of its optimization parameter regardless of signal-to-noise ratio variations between 2 to 0.8.**

I. Introduction

THE detection of radiological material in motion forms a burning issue when addressing CBRN threats [1]. Whether the potential carrier may be a pedestrian, a train or a vehicle, Radiation Portal Monitors (RPM) are deployed and sized so that the large-volume sensor inserted into the device is found as close as possible to the radioactive source path. The alarm of the detector is triggered as soon as the relevant signal rises over a given threshold, which is set with regards to the amplitude of the background activity as well as to some assumptions formulated on the laws followed by the different signals.

II. Related Work

Classical industrial detection systems for moving sources perform the detection by mere signal amplitude triggering on a recording channel interfaced with a radiation sensor. For the detection to be efficient when the carrier is in motion, a large volume sensor is supplied, typically a gas or plastic scintillator for scalability and cost-effectiveness reasons [2-3]. To obtain significant gains in the richness of the information provided by such a single RPM, *ad hoc* strategies have been developed. Guillot et al. have, for instance, described and patented [4] a method for the detection and identification of moving sources using a spectrometry device, which lies outside the scope of the present paper, focused on pure detection applications. To increase the sensitivity of the detection, especially critical under low signal-to-noise ratios (*SNR*, for which we hereby use the classical definition of the source signal count divided by the square root of the background fundamental count), energy windowing strategies have been introduced. Robinson et al. [5] compare at each time the observed spectrum to adequately chosen energy windows over a background previously acquired at the RPM level. To maximize the gain in sensitivity, Vilim et al. [6] select the energy ranges providing the highest *SNR* values. It then follows that such methods are highly dependent on the energy resolution of the provided spectrometric information. Hence the quest for alternative methods when dealing with large-scale plastic scintillators exhibiting high detection efficiencies but mediocre energy resolutions.

A powerful strategy to address sensitivity issues when dealing with challenging *SNR* moving sources lies within the deployment of not only one RPM, but a network of such sensors. While independent multichannel triggering remains available for such a network, the measurement then being computed by the logical summation of all channel detection answers, some valuable information may be extracted by analyzing the delayed temporal evolution of the signals recorded in front of the respective RPM. Such networks, of variable geometries and dimensions, are particularly praised for source localization problematics, in which they typically appear two-dimensional (2-D) and large-scale. Dedicated algorithms have then been elaborated to track the source trajectory without prior knowledge, as carried out with Markov Chains calculations and Bayesian methods by Brennan et al. [7] or triangulation by Chin et al. [8]. Such highly iterative and finely optimized methods are poorly suited for typical CBRN issues dealing with straight trajectories of pedestrian or vehicle source carriers under real time, immediate response constraint. Alternatively, faster algorithms have been proposed: Nemzek et al. [9] describe a method based on the combination of different channels and final comparison to the signal of a single chosen RPM. Stephens et al. [10] additionally justify a preliminary probabilistic triggering on the acquisition channels. Both these methods nevertheless impose for the speed of the source carrier to be known with a certain degree of precision, which in real life situations is uneasy to achieve and may thus constitute an excessive constraint for the detection system conceiver. Sundaresan et al. [11] have, on the other hand, set up a measurement based on *a priori* independent multichannel detections which are all correlated *a posteriori* to lower the false alarm probability. Such an approach, as firstly based on a single channel variation monitoring, does not allow for any

Jonathan Dumazert, Romain Coulon, Vladimir Kondrasovs, Karim Boudergui, Guillaume Sannié, Jordan Gameiro and Stéphane Normand are with CEA, LIST, Laboratoire Capteurs et Architectures Electroniques, 91191 Gif-sur-Yvette, France (telephone: +33(0)169085324, e-mail: jonathan.dumazert@cea.fr).

Laurence Méchin is with CNRS (UMR6072), UCBN, ENSICAEN, Groupe de Recherche en Informatique, Image, Automatique et Instrumentation de Caen, 14050 Caen, France.

sensitivity improvement of the system, so that the false alarm reduction does not reveal itself sufficient to operate the detector under challengingly low *SNR*.

Coulon et al. have described and patented [12-13] an alternative exploitation of the compared temporal information contained in the different recording channel memories. As the source carrier, supposedly following a linear or quasi linear trajectory, successively passes in front of each of the RPM, displayed in a network, it induces for a short time an increase in the signal level. Such an increase, in the cases of challenging *SNR*, may be impossible to detect in front of the first RPM among the inherent level of fluctuations induced by the Poisson statistical nature of the measured radiation background. Nevertheless, supposing that the carrier moves at constant speed or quasi constant speed along the network (which forms a more versatile assumption than the one of a *precisely determined constant* speed and a reasonable one for a pedestrian, a car or a train before its final deceleration), an echo of the undetected additional signal may be found on every other channel and, as the speed is constant, these successive appearances are periodic. It is therefore possible to search for a temporal delay, on the form of a multiple value of the fundamental sampling time step, which will, to the maximum possible extent, superimpose the successive echoes of the undetected signal increases and exploit the multiplied values of these echoes as the significant variation to be detected, by a specified amplitude triggering, among the inherent fluctuations of a computed temporal multiplication vector. Coulon et al. have calibrated a hypothesis test for moving source detection without any assumption made on the expected nature and intensity of such a product vector, making use of the empirical estimates for the mean and standard deviation of the vector. Their approach has proven itself efficient for a relatively high speed (7 $m.s^{-1}$) low count rate (12 cps) source among a challenging count rate background (20 cps). The authors of the present paper propose to investigate an upgrade of the detection test introduced by Coulon et al., first describing the underlying statistics governing the temporal product vector used for the test, and then parametrizing the said test by a novel expectation and widening as computed under the assumption of a product of Poisson laws.

III. Mathematical formalism

Let us consider the signals registered on the two RPM of a given linear network to be generated by two real and independent underlying random variables S_1 and S_2 with Poisson density laws respectively parametrized by λ_1 and λ_2. Providing λ_1 and λ_2 are high enough, both distributions may be approached by the normal distributions $\mathcal{N}(\lambda_1, \lambda_1)$ and $\mathcal{N}(\lambda_2, \lambda_2)$. We consider the aleatory variable $Y = S_1 \cdot S_2$ formed by the product of both previous ones.

A. Calculation of the expected value and variance of Y

The expected value $E[Y]$ of the random variable formed by the product of two real and independent variables is given by the product of both expected values $E[S_1]$ and $E[S_2]$ of the considered variables:

$$E[Y] = E[S_1 \cdot S_2] = E[S_1] \cdot E[S_2] = \lambda_1 \cdot \lambda_2 \quad (1)$$

The variance $V(Y)$ of Y is a function of both variances $V(S_1)$ and $V(S_2)$ of the multiplied variables, as well as of their expected values $E[S_1]$ and $E[S_2]$:

$$V(Y) = V(S_1) \cdot V(S_2) + V(S_1) \cdot (E[S_2])^2 + V(S_2) \cdot (E[S_1])^2$$
$$V(Y) = \lambda_1 \cdot \lambda_2 \cdot (1 + \lambda_1 + \lambda_2) \quad (2)$$

B. Generalization to the product of n variables

The previous formalism may be generalized to the case of a linear network displaying any number *n* of RPM. Let us then consider *n* real and independent random variables S_1, $S_2 \ldots$ S_n with Poisson density laws respectively parametrized by $\lambda_1, \lambda_2 \ldots \lambda_n$, which are respectively approached by the normal law distributions $\mathcal{N}(\lambda_1, \lambda_1)$, $\mathcal{N}(\lambda_2, \lambda_2) \ldots \mathcal{N}(\lambda_n, \lambda_n)$. We consider the random variable $Y = S_1 \cdot S_2 \ldots S_n$ formed by the product of the *n* previous ones.

The expected value $E[Y]$ of the variable defined as the product of *n* real and independent variables is given by the product of the expected values $E[S_1]$, $E[S_2] \ldots$ $E[S_n]$ of the considered variables:

$$E[Y] = E[S_1] \cdot E[S_2] \ldots E[S_n] = \lambda_1 \cdot \lambda_2 \ldots \lambda_n = \prod_{i=1}^{n} \lambda_i \quad (3)$$

The calculation of the variance $V(Y)$ of Y is carried out by applying recursively the result of *III.A.*:

$$V(Y) = V(S_1 \cdot S_2 \ldots S_{n-1}) \cdot V(S_n) + V(S_1 \cdot S_2 \ldots S_{n-1}) \cdot (E[S_n])^2 + V(S_n) \cdot (E[S_1 \cdot S_2 \ldots S_{n-1}])^2$$
$$V(Y) = V(S_1 \cdot S_2 \ldots S_{n-1}) \cdot (\lambda_n + \lambda_n^2) + \lambda_n \cdot \left(\prod_{i=1}^{n-1} \lambda_i \right)^2 \quad (4)$$

The same treatment is then applied to the variables $S_1 \cdot S_2 \ldots S_{n-1}$, then $S_1 \cdot S_2 \ldots S_{n-2}$ ..., lowering the number of factors after every iteration until only 2 remain and we are therefore brought back to the case dealt with in *III.A*.

IV. Method

This section divulges the steps followed by the simulation algorithm to assess the respective performances of different algorithms for the detection of a radiation moving source passing in front of *n* equidistant RPM displayed in a linear network.

A. Simulation of the radiation signal, time depth and memory buffer management

Let the number of RPM displayed be labeled *n*, the distance between the network line and the source carrier d_1, the distance between two adjacent detectors d_2, the carrier speed

v, which is supposed to be constant or negligibly varying for the type of applications we are aiming at, the background radiation count rate λ_b and the source count rate in front of one detector λ_s. The instantaneous count rate $\lambda_j[t_i]$ which is expected to be registered at the i^{th} integration time step by the j^{th} RPM detector, described as a function of the time-dependent source carrier position $x[t_i]$, is provided by (5). The calculation has been carried out under the approximation that the source and the detector may be modeled by their centers of mass and therefore that the principle of the ratio of solid angles applies.

$$\forall j \in [\![1;n]\!], \forall i \in [\![1;M]\!], \quad \lambda_j[t_i] = \frac{\lambda_s \cdot d_1^2}{d_1^2 + (x[t_i] - x_j)^2} + \lambda_b \tag{5}$$

The recording time step is designated as $\Delta t = t_{i+1} - t_i$. Given the introduced notations, the *SNR* is evaluated as stated in (6):

$$SNR = \frac{\lambda_s \cdot \Delta t}{\sqrt{\lambda_b \cdot \Delta t}} = \frac{\lambda_s \cdot \sqrt{\Delta t}}{\sqrt{\lambda_b}} \tag{6}$$

For each of the *j* RPM channel, a time-varying count is generated following an inhomogeneous Poisson process modeled with the use of the "Poissrnd" $\wp$ pseudo-random function of Matlab parametrized by the time-varying value of the underlying count rate λ_j. A third-order moving averaging $MA(.,3)$ is applied to the count rate vector previous to any further operation, so that the expectation for the recorded signal $S_j[t_i]$ at the i^{th} integration time step by the j^{th} RPM detector is provided by (7).

$$\forall j \in [\![1;n]\!], \forall i \in [\![1;M]\!], \quad S_j[t_i] = MA(\wp(\lambda_j[t_i] \cdot \Delta t), 3) \tag{7}$$

For every *j* channel and every discrete time step t_i a new value is recorded in a signal matrix $(S_{i,j} = S_j[t_i])_{i=1\dots M, j=1\dots n}$, where *M* represents the time depth of the recording and the memory buffer size allocated at every independent detector level.

B. Calculation of the correlation vector

Both the hypothesis test divulged by Coulon et al., which is assumption-free on the distributions followed by the radiation signals, and the one we introduce in this paper, based on a Poisson law assumption, make use of the same temporal product vector $(R_k)_{k=1\dots N_R}$ of length $N_R = \left\lfloor \frac{n}{M} \right\rfloor$. The k^{th} term of the product vector is calculated as described in (8) and (9) for $n = 2$ and $n = 4$ respectively:

$$\forall k \in [\![1;N_R]\!], R_k = \max_{i \in [\![1;M-k+1]\!]} (S_{i,1} \cdot S_{i+k-1,2}) \tag{8}$$

$$\forall k \in [\![1;N_R]\!], \quad R_k = \max_{i \in [\![1;M-4(k-1)]\!]} (S_{i,1} \cdot S_{i+k-1,2} \cdot S_{i+2(k-1),3} \cdot S_{i+4(k-1),4}) \tag{9}$$

C. Hypothesis tests for the detection

Any of the benchmarked hypothesis tests for the detection of a radiative source is based on the comparison between a registered signal and a decision threshold set with regards to both the expected amplitude and the distribution of the signal around this expected amplitude.

The simplest hypothesis test only makes use of one RPM, say the first in the network. If we define H_0 as the assertion "no source is passing in front of the RPM network" and H_1 as the assertion "a source is passing in front of the RPM network", the acceptance of H_1 is parametrized by a coverage factor K according to (10) so that if:

$$\max_{i \in [\![1;M]\!]} (S_{i,1}) > \overline{S_{\cdot,1}} + \mathrm{K} \cdot \sigma(S_{\cdot,1}) \tag{10}$$

then the alarm is triggered and a source is detected. The estimator of the expected value $\overline{S_{\cdot,1}}$ and the estimator of the standard deviation $\sigma(S_{\cdot,1})$ over the count rate vector are respectively calculated with the formulae displayed in (11) and (12):

$$\overline{S_{\cdot,1}} = \frac{1}{M} \sum_{i=1}^{M} S_{i,1} \tag{11}$$

$$\sigma(S_{\cdot,1}) = \sqrt{\frac{1}{M-1} \sum_{i=1}^{M} (S_{i,1} - \overline{S_{\cdot,1}})^2} \tag{12}$$

The factor K is investigated with regards to the best compromise between false alarm probability ($P_{FA} = P(\mathrm{H}_1|\mathrm{H}_0)$ by definition), which corresponds to the acceptance of H_1 in the absence of a moving source ($\lambda_s = 0$) and the detection probability ($P_D = P(\mathrm{H}_1|\mathrm{H}_1)$ by definition), which represents the acceptance of H_1 in the presence of a source. This compromise may be figured by Receiver Operating Characteristic [14] (ROC) plotting the evolution of P_D as a function P_{FA} or, if no critical P_{FA} has been previously defined for the benchmark, by the evolution of the intuitive factor of merit labeled *FOM* and trivially calculated following (13):

$$FOM = P_D - P_{FA} \tag{13}$$

Under unfavorable *SNR*, the canonic strategy, which consists in triggering the alarm whenever the hypothesis test defined in (9), for a preset value of K, results in the acceptance at the level of any of the *n* RPM displayed in the network (OR logical function), results in unacceptably low *FOM* values, as Coulon et al. have already demonstrated. Hence the development of alternative hypothesis tests based on the superimposition of the signals registered on all channels, as built in the temporal product vectors.

The hypothesis test we wish to benchmark the new algorithm disclosed in this paper to adds one acceptance condition for H_1 in the OR logical function over the *n* independent tests introduced *supra*, which is stipulated in (14):

$$\max_{k \in [\![1;N_R]\!]} (R_k) > \overline{R_\cdot} + \mathrm{K} \cdot \sigma(R_\cdot) \tag{14}$$

The estimator of the expected value $\overline{R_\cdot}$ and the estimator of the standard deviation $\sigma(R_\cdot)$ over the temporal product vector are respectively calculated with the formulae displayed in (15) and (16):

$$\overline{R_{\cdot}} = \frac{1}{N_R}\sum_{k=1}^{M} R_k \tag{15}$$

$$\sigma(R_{\cdot}) = \sqrt{\frac{1}{N_R - 1}\sum_{i=1}^{N_R}(R_k - \overline{R_{\cdot}})^2} \tag{16}$$

The factor K is investigated with regards to the optimal tradeoff represented by the maximization of *FOM*.

The concept of the alternative algorithm introduced in this paper lies within the replacement of $\overline{R_{\cdot}}$ and $\sigma(R_{\cdot})$ by estimations of the expected value and variance of the correlation vector based on the theoretical derivation of section *III*, hence making use of the knowledge of the Poisson nature of the underlying laws to the registered count rates. In this alternative hypothesis test, the additional acceptance condition for H_1 in the OR logical function over the n independent tests writes as described in (17) and (18) for $n = 2$ and $n = 4$ respectively, deduced from (1) to (4):

$$\max_{k\in[\![1;N_R]\!]}(R_k) > \overline{S_{\cdot,1}}\cdot\overline{S_{\cdot,2}} + \mathrm{K}\cdot\sqrt{\overline{S_{\cdot,1}}\cdot\overline{S_{\cdot,2}}\cdot\left(1+\overline{S_{\cdot,1}}+\overline{S_{\cdot,2}}\right)} \tag{17}$$

$$\max_{k\in[\![1;N_R]\!]}(R_k) > \prod_{j=1}^{4}\overline{S_{\cdot,J}} + \mathrm{K}\cdot\sqrt{\Pi\cdot\left(\overline{S_{\cdot,4}}+\overline{S_{\cdot,4}}^2\right)+\overline{S_{\cdot,4}}\cdot\left(\prod_{j=1}^{3}\overline{S_{\cdot,J}}\right)^2} \tag{18}$$

where the factor Π is calculated as made explicit in (19):

$$\Pi = \overline{S_{\cdot,1}}\cdot\overline{S_{\cdot,2}}\cdot\left(1+\overline{S_{\cdot,1}}+\overline{S_{\cdot,2}}\right)\cdot\left(\overline{S_{\cdot,3}}+\overline{S_{\cdot,3}}^2\right)+\overline{S_{\cdot,3}}\cdot\left(\overline{S_{\cdot,1}}\cdot\overline{S_{\cdot,2}}\right)^2 \tag{19}$$

For every j channel, the expected count value $\overline{S_{\cdot,J}}$ is evaluated according to (20):

$$\forall j \in [\![1;n]\!], \overline{S_{\cdot,J}} = \frac{1}{M}\sum_{i=1}^{M} S_{i,j} \tag{20}$$

The factor K is once again varied until the maximum value for *FOM* is found.

V. Results

A. Assessment scheme

To access the characteristic representing the evolution of *FOM* as a function of the coverage factor K, in the four previously introduced configurations of implementation, we generate for every of these situations and every *SNR* value considered in them, a number $N = 1000$ times the activity λ_s we wish to detect and the same $N = 1000$ times a null activity $\lambda_s = 0$ to evaluate the false alarm probability in the described background and detection scheme. If we denote N_D the number of detection cases in the first simulation batch (non-null activity) and N_{FA} the number of detection cases in the second batch (null activity), then the quantities P_D and P_{FA} defined in *IV.C.*, with their respective standard deviations $\sigma(P_D)$ and $\sigma(P_{FA})$ (quantifying the repeatability uncertainty lying upon them), are estimated as shown in (21) to (24).

$$P_D = \frac{N_D}{N} \tag{21}$$

$$\sigma(P_D) = \sqrt{\frac{1}{N}\cdot P_D\cdot(1-P_D)} \tag{22}$$

$$P_{FA} = \frac{N_{FA}}{N} \tag{23}$$

$$\sigma(P_{FA}) = \sqrt{\frac{1}{N}\cdot P_{FA}\cdot(1-P_{FA})} \tag{24}$$

Ultimately the performance indicator *FOM* is evaluated as the difference between P_D and P_{FA}, and its associated uncertainty $\sigma(FOM)$ is computed as exhibited on (25).

$$\sigma(FOM) = \sqrt{\sigma^2(P_D)+\sigma^2(P_{FA})} \tag{25}$$

The number of iterations $N = 1000$ has been set so that, for all the results presented in subsections *V.B.* to *V.E.*, the overall uncertainty $\sigma(FOM)$ never exceeds the value of 0.02 (2%). The recording time step $\Delta t = t_{i+1} - t_i$and the buffer size M, which are both fixed parameters for all simulations whose results are divulged in the four following subsections, are respectively set to 0.1 s and 100, which are compatible with the constraint of a quasi-continuous monitoring of radioactivity.

B. Pedestrian carrier with high count rate background

The first real-life challenging situation we intend to simulate is that of a RPM network displayed to detect a radioactive source carried by a pedestrian with a usually high count rate background (for instance nearby a facility dedicated to the storage and handling of sources for research purposes, which is the typical background encountered during the first experimental assessment of a new detection sensor and/or algorithm or an environment of critical interest for radioprotection issues, and with large-scale RPM sensors). The value chosen for the background count rate $\lambda_b = 2000$ cps. A realistic value for the speed of the pedestrian, who is to walk alongside the detector network at a distance $d_1 = 1$ m, is set at $v = 5$ km.h^{-1}. As this speed is low, so is the spacing between adjacent RPM in the line, which is put equal to $d_2 = 2$ m. The *FOM* value is computed and displayed on Fig. 1 to Fig. 4 for four increasing challenging values of signal-to-noise ratios: $SNR = 2$, $SNR = 1.5$, $SNR = 1$ and $SNR = 0.8$. On every figure, we have superimposed, with their respective optimization ranges with regards to K, the values of *FOM* obtained for an independent detection on the first RPM (M1FOM), for a detection using the product vector and empirical mean and variance as done by Coulon et al. with a linear network of $n = 2$ (R2FOM) and $n = 4$ (R4FOM) RPM respectively, and for a detection using the product vector and a Poisson hypothesis on the mean and variances as

disclosed in this paper with a linear network of $n = 2$ (PG2FOM) and $n = 4$ (PG4FOM) RPM respectively.

C. *Pedestrian carrier with low count rate background*

The second real-life challenging situation we intend to simulate is that of a small or moderate-size sensor network (typically 1 to 10 cm height and diameter) displayed to detect a radioactive source once again carried by a pedestrian, though this time with a usually very low count rate background (as in most typical CBRN applications). The value chosen for the background count rate $\lambda_b = 5$ cps is additionally specified as extremely low so that the present study may cover the range defined by Coulon et al. (20 cps). The values $d_1 = 1$ m, $v = 5$ km.h^{-1} and $d_2 = 2$ m, well suited for the monitoring of a flow of pedestrians, remain unchanged from the *V.B.* settings. Fig. 5 to Fig. 8 display the same characteristics of *FOM* as a function of K as those disclosed in *V.B.*, where the activity λ_s is set to simulate the same four values of *SNR* and where the same five detection tests are assessed.

VI. Discussion

The characteristics displayed in Fig. 1 to Fig. 8 do not include an independent multichannel test over $n = 2$ and $n = 4$ RPM, for its performance usually does not significantly differ from the ones of M1FOM, except for $SNR = 2$ which represents the least challenging case and thus the least relevant for the present comparative study.

The first conclusions drawn from the simulation results converge to corroborate the claims made in Coulon et al. about the general merits of temporal multiplication, regardless of the chosen hypothesis test. In both configurations (pedestrian with $\lambda_b = 2000$ cps, pedestrian with $\lambda_b = 5$ cps), the exploitation of the echo allows a drastic improvement of the *FOM* value under low *SNR* conditions, almost systematically reaching a 10 % to 20 % increase from M1FOM to R2FOM or PG2FOM, and 30 % to 40 % increases from M1FOM to R4FOM to PG2FOM. Our results additionally confirm that, for both hypothesis tests making use of the temporal product vector, the performances increase with the number of RPM displayed in the network. We have therefore widened the promising conclusions of Coulon et al. from a particular configuration suiting a vehicle carrier in a relatively low count rate background to a larger spectrum of concrete applications.

The core of this paper lies within the two-by-two comparisons of the characteristics of R2FOM and PG2FOM one the hand, and R4FOM and PG4FOM on the other hand, as PG2FOM and PG4FOM result from the original hypothesis test hereby disclosed and described in (17) to (20). The most obvious observation from Fig. 1 to Fig. 8 is that the maximum of the PG2FOM is constantly superior to the maximum of R2FOM, and similarly that the maximum of PG4FOM exceeds the maximum of R4FOM. The discrepancy between PG4FOM and R4FOM is particularly noticeable under $\lambda_b = 5$ cps background. As any of the chosen tests for the detection of moving source should be set without prior knowledge of the *SNR*, the stability of the value for the coverage factor K providing the best *FOM* is another critical figure of merit. A superficial look at the characteristics reveals that the optimization range for K differs greatly for the test making use of the empirical mean and variance and our test under Poisson assumption. The distributions of R2FOM and R4FOM exhibit extremely smooth profiles around their maximum with low count rate background, as it had already been reported by Coulon et al., which guarantees a high degree of robustness of the test for a value of K chosen in the most important *FOM* values area and a *SNR* varying between 2 and 0.8. The characteristics of PG2FOM and PG4FOM are sharper around their maximum value, but still ensure a robust detection setting for varying *SNR*. For instance, Fig. 1 to Fig. 4 show that an initial setting of $K = 3$ guarantees PG4FOM values of respectively 0.83, 0.85, 0.78 and 0.63 for $SNR = 2$, $SNR = 1.5$, $SNR = 1$, and $SNR = 0.8$, which are both satisfactory in absolute terms given the unfavorable *SNR* under which they are obtained and also superior to the concurrent performances disclosed by the R4FOM characteristics over the same *SNR* range.

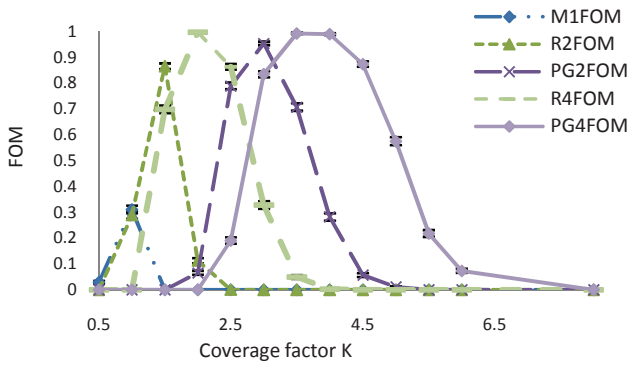

Fig. 1. Pedestrian ($\lambda_b = 2000$ cps; $SNR = 2$).

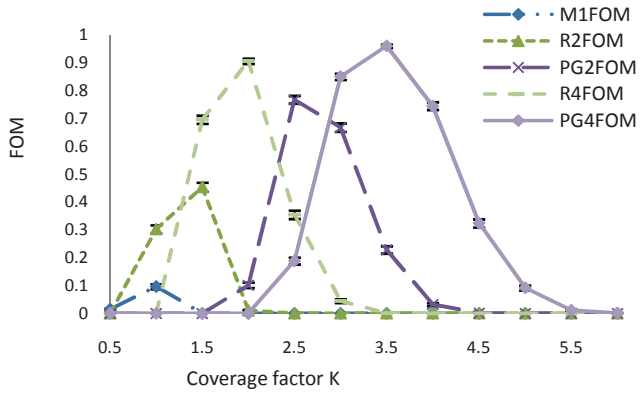

Fig. 2. Pedestrian ($\lambda_b = 2000$ cps; $SNR = 1.5$).

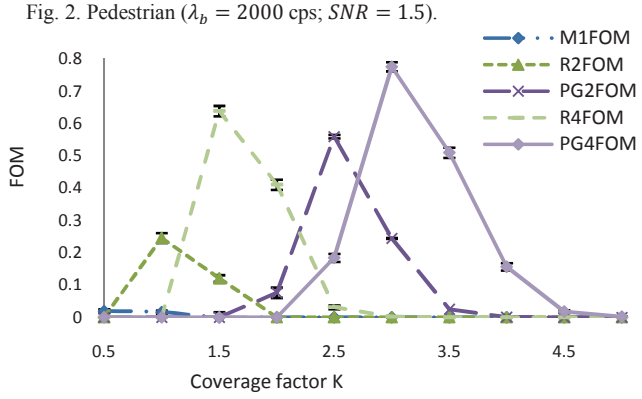

Fig. 3. Pedestrian ($\lambda_b = 2000$ cps; $SNR = 1$).

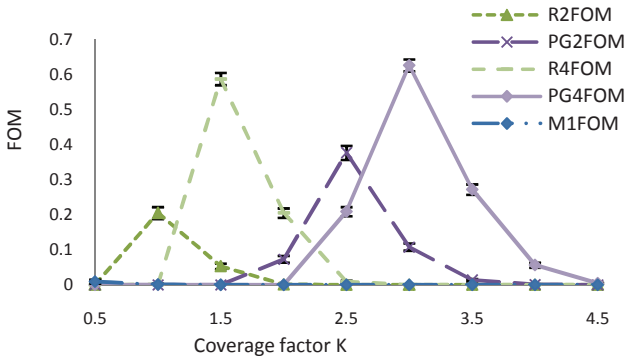

Fig. 4. Pedestrian ($\lambda_b = 2000$ cps; $SNR = 0.8$).

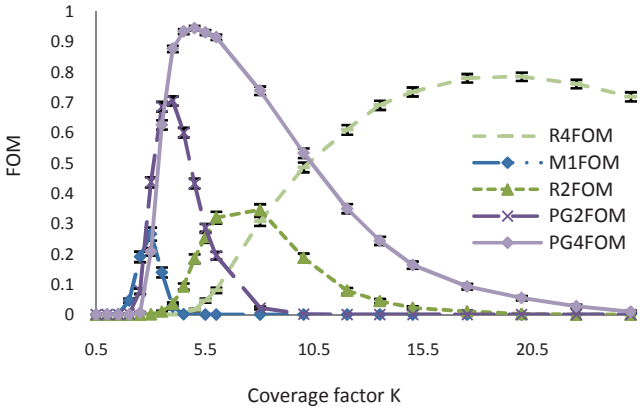

Fig. 5. Pedestrian ($\lambda_b = 5$ cps; $SNR = 2$).

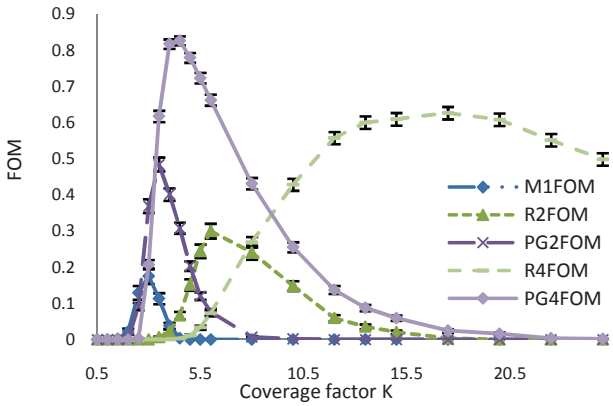

Fig. 6. Pedestrian ($\lambda_b = 5$ cps; $SNR = 1.5$).

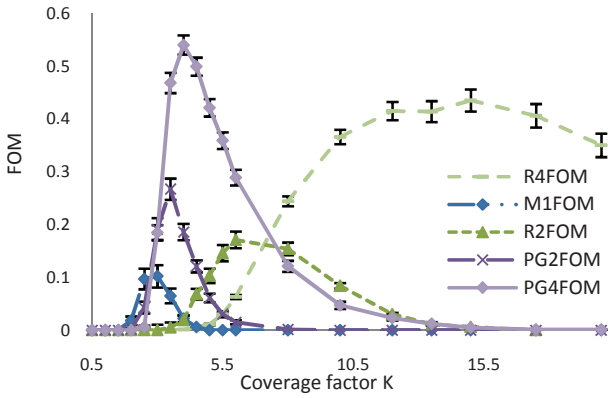

Fig. 7. Pedestrian ($\lambda_b = 5$ cps; $SNR = 1$).

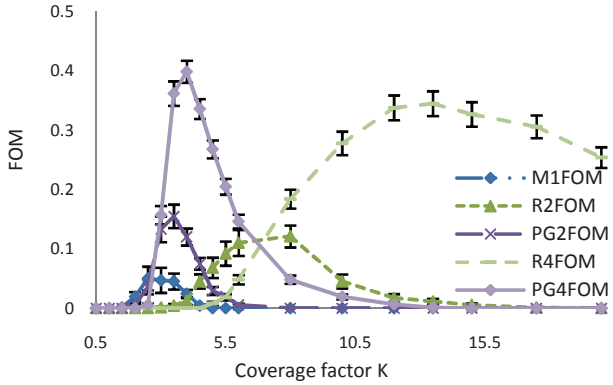

Fig. 8. Pedestrian ($\lambda_b = 5$ cps; $SNR = 0.8$).

VII. Conclusions

The simulation study in realistic radioactive backgrounds and source carrier configurations conducted in this paper has allowed us to validate the concept of a new hypothesis test for the detection of a constant speed moving sources under challenging signal-to-noise ratios (from 2 down to 0.8). This test, which makes use of Poisson law assumptions, known to govern the generation of a radioactive process, for the estimation of expected mean and variance of a temporal product vector, has proven itself able to ensure a better tradeoff between detection sensitivity and false alarm susceptibility than its previously introduced alternative, based solely on the empirical mean and variance of the product vector. Such significant improvement in the sensitivity/false alarm compromise of the detection has been reached without any degradation of the robustness of the test, as its optimization range remains consistent, for a given background, under varying *SNR*.

Among major limitations to the benchmarked algorithms, two are common to the test disclosed in Coulon et al. and the one introduced in this paper. Firstly, the optimal coverage factor must be set with regards to a previously known value for the recorded background radiation activity. Secondly, the source has to move with a constant speed, or at least a non-significantly varying one, along the RPM line for the product vector, as hereby calculated, to enable the exploitation of the echo. Our next exploration for improvements will then be orientated toward the softening of this constraint, for instance replacing the condition of constant speed, better suited for pedestrian applications than for the monitoring of a train entering a station, by a condition of speed decreasing according to a constant gradient. The second main limitation only concerns the hypothesis test introduced in this paper, which, by definition, becomes ineffective when the signals registered on the different RPM diverge from the ones that could be reconstructed using a Poisson law model. Such distortion may for instance arise in the presence of pile-up at the acquisition electronics level, and would, once diagnosed, impose the use of the empirical mean and variance in the detection hypothesis test.

The detection algorithm described in this article, together with the one presented in Coulon et al., is to be implemented into a prototype system developed in the course of the SECUR-ED European project for urban mass transportation [15]. Each RPM sensor of the network is made of two $10 \times 10 \times 100$ cm plastic scintillators of EJ-200 type produced

by Eljen Technology. A demonstration campaign will be thoroughly conducted to ensure the compliance of both the sensor device and the detection algorithms to the international standards [16] labeled ANSI N42.35.

ACKNOWLEDGEMENTS

The authors would like to thank the members of the SECUR-ED consortium for having implicated them in their research.

REFERENCES

[1] "Chemical, biological, radiological or nuclear (CBRN) detection: a technological overview", NATO Parliamentary Assembly (2005).
[2] "RADOS DnD-Portal," MIRION Technologies Technical file (2010).
[3] "Radiological control of vehicle load," SAPHYMO Technical file 29294 835 EN (2011).
[4] L. Guillot, A. Reboli and A. Dominique, "Dispositif et procédé de détection et d'identification en temps réel d'une source radioactive en mouvement" (2008).
[5] S. M. Robinson, S. E. Bender, E. L. Flumerfelt, C. A. Lopresti and M. L. Woodring, "Time series evaluation of radiation portal monitor data for point source detection," *IEEE Trans. Nucl. Sci.,* **56**, *6,* pp. 3688-3693 (2009).
[6] R. B. Vilim, R. Klann, C. Fink, C. Campos and T. Medley, "Sensitivity improvement in low-profile distributed detector systems for tracking sources in transit," *Proc. IEEE Conf. Technol. Homeland Security*, p. 174-179 (2007).
[7] S. Brennan, A. Mielke and D. Torney, "Radioactive source detection by sensor networks," *IEEE Trans. Nucl. Sci.,* **52**, *3,* pp. 813-819 (2005).
[8] J.-C. Chin, N. Rao, D. Yau, M. Shankar, Y. Hou, J. Hou, S. Srivathsan and S. Iyengar, "Identification of low-level point radioactive source using a sensor network," *AMC Trans. Sensor Netw.,* **7**, *3,* pp. 1-21, 35 (2010).
[9] R Nemzek, J. Dreicer, D. Torney and T. Warnock, "Distributed sensor networks for detection of mobile radioactive sources," *IEEE Trans. Nucl. Sci.,* **51**, *4,* pp. 1693-1700 (2004).
[10] D. Stephens and A. Peurrung, "Detection of moving radioactive sources using sensor networks," *IEEE Trans. Nucl. Sci.,* **51**, *5,* pp. 2273-2278 (2004).
[11] A. Sundaresan, P. K. Varshney and N. S. V. Rao, "Distributed detection of a nuclear radioactive source using fusion of correlated decisions," *Proc. Int. Conf. Infor. Fusion,* pp 1-7 (2007).
[12] R. Coulon, V. Kondrasovs, S. Normand and M. Bakkali, Commissariat à l'Energie Atomique et aux Energies Alternatives, "Procédé de détection de source radioactive en mouvement et dispositif associé" (2014).
[13] R. Coulon, V. Kondrasovs, K. Boudergui and S. Normand, "Moving sources detection algorithm for radiation portal monitors used in a linear network," *IEEE Trans. Nucl. Sci.,* **61**, *4*, pp. 2189-2194 (2014).
[14] G. Knoll, *Radiation Detection and Measurement*, Fourth Edition, John Wiley & Sons, Inc., pp. 94-95 (1999).
[15] K. Boudergui, V. Kondrasovs, R. Coulon, G. Corré and S. Normand, "New monitoring system to detect a radioactive material in motion," *Proc. ANIMMA* (2013).
[16] "American national standard for evaluation and performance of radiation detection portal monitors for use in homeland security," ANSI 42.35 (2006).bricc.anu.edu.au/index.php